LONGWAVE ELECTRON OSCILLATIONS IN A BEAM-PLASMA SYSTEM

M. V. NEZLIN, G. I. SAPOZHNIKOV and A. M. SOLNTSEV

Submitted to JETP editor August 27, 1965

J. Exptl. Theoret. Phys. (U.S.S.R.) **50**, 349–363 (February, 1966)

In this paper we report on an experimental investigation of longwave electron oscillations excited by an electron beam in a low-density plasma confined by a strong longitudinal magnetic field. The plasma is produced as a result of ionization induced by the beam, the gas pressure being approximately 10^{-5} mm Hg; the plasma density is comparable with the beam density. The oscillations observed in these experiments are not plasma oscillations; the characteristic oscillation spectrum consists of a series of harmonics whose wavelengths (λ_n) are governed by the relation $\lambda_n = 2L/n$ (n is the harmonic number and L is the length of the beam) while the frequencies ω_n are determined by the velocity of the electron beam (v) and the wavelength: $\omega_n \sim k_n v$ where $k_n = 2\pi/\lambda_n$. It is shown that the conditions appropriate to the excitation of the oscillations, and the spectral characteristics, are in good agreement with the theory of longitudinal electron oscillations in a uniform beam-plasma system which is bounded in the longitudinal and transverse directions.

INTRODUCTION

OF the large variety of oscillations possible in a uniform plasma[1-7] perhaps the greatest popularity has been received by the longitudinal electron oscillations. These oscillations are typically excited by an electron beam whose density n_1 is small compared with the plasma density n_2.[8] The excitation condition coincides with the criterion for Cerenkov radiation of plasma waves $\omega = kv$, where ω is the angular frequency of the oscillations, $k = 2\pi/\lambda$ is the wave number, and v is the beam velocity. Depending on the relation between the wavelength λ and the transverse dimensions of the beam (radius) r_0 the oscillation frequency ω can either be equal to the electron-plasma frequency ω_p or considerably lower than ω_p:[3-7]

$$\omega = \begin{cases} (4\pi n_2 e^2/m)^{1/2} = \omega_p & \text{for} \quad \lambda \ll r_0 \\ \dfrac{\omega_p}{\sqrt{2}} kr_0 \ln \dfrac{1}{kr_0} \ll \omega_p & \text{for} \quad \lambda \gg r_0 \end{cases}$$

In contrast with these oscillations, which are characterized by spectra with single frequencies, there exist oscillations whose spectra contain a series of harmonics. These oscillations (which are also longitudinal electron oscillations and are also beam-excited) are to be associated with wavelengths.

$$\lambda_n = 2L/n, \quad n = 1, 2, 3, \ldots \tag{1}$$

(L is the beam length) and frequencies ω_n given by the relation

$$\omega_n = Ck_n v, \tag{2}$$

where $k_n = 2\pi/\lambda_n$ while C is a coefficient whose meaning will be developed below.

The present work is devoted to a study of these oscillations. The experiments reported herein indicate that the excitation of these oscillations requires a certain combination of conditions which usually hold in an electron beam of finite length propagating in vacuum ($p \approx 10^{-4} - 10^{-6}$ mm Hg) so long as the beam current exceeds some critical value which depends on plasma density and the beam velocity. It should be noted that the work reported here is not the first in this field. Experimental investigations of high-frequency oscillations in electron-beams propagating in vacuum have been reported earlier by a number of authors (cf. for example [9,10]). However, the data on the oscillation spectrum reported in this earlier work were not systematic and thus could not give a definitive description of the oscillations.

The present work has been undertaken in order to perform a systematic investigation of the spectra of these oscillations, to investigate their characteristics, and to study the excitation mechanism.

1. EXPERIMENTAL ARRANGEMENT

The investigation of oscillations in an electron-beam has been carried out using the apparatus shown schematically in Fig. 1.

A beam of electrons is emitted by a plane tungsten cathode which is indirectly heated and which

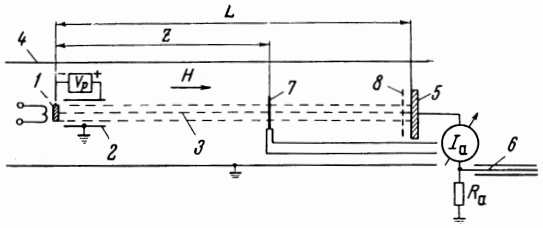

FIG. 1. Experimental arrangement: 1) Cathode, 2) accelerating electrode (discharge chamber), 3) electron beam, 4) vacuum chamber, 5) movable anode (beam collector), R_a measurement resistance (13 ohms), 6) measurement cable, 7) probe, 8) grid.

is 1 cm in diameter; these electrons are accelerated to an energy of several tens of electron volts and propagate along a strong magnetic field in an equipotential space along the axis of a cylinder with metal walls (30 cm in diameter) and then finally reach a movable anode. The beam length can be varied from 16 to 150 cm, the pressure (hydrogen) can be varied from $10^{-4}-10^{-6}$ mm Hg and the magnetic field can be varied up to 1–5 $\times 10^3$ G. In these experiments we measure the oscillation spectrum of the electron current at the anode and on a Langmuir probe 40 mm in diameter and 0.8 mm in diameter which is translated along a diameter of the beam which can be moved along the axis of the beam as well (when the anode current is measured the probe is retracted from the beam).

The oscillation measurements are carried out as follows: The signal across the measurement resistance (for example R_a in Fig. 1) is fed to a coaxial cable and a matched load and then to the input of a panoramic spectrum analyzer (S 4–8), on the screen of which there appears a spectrum giving the amplitude as a function of frequency (linear scales along both axes). The current oscillations at the probe are measured at zero probe potential (zero potential is taken to be the potential of the grounded chamber walls); these are found to be completely similar to the current oscillations in the anode circuit.

In one of the experiments a grounded metal grid is placed in front of the anode in order to inhibit secondary electron emission; in this case a variable positive potential is applied to the anode.

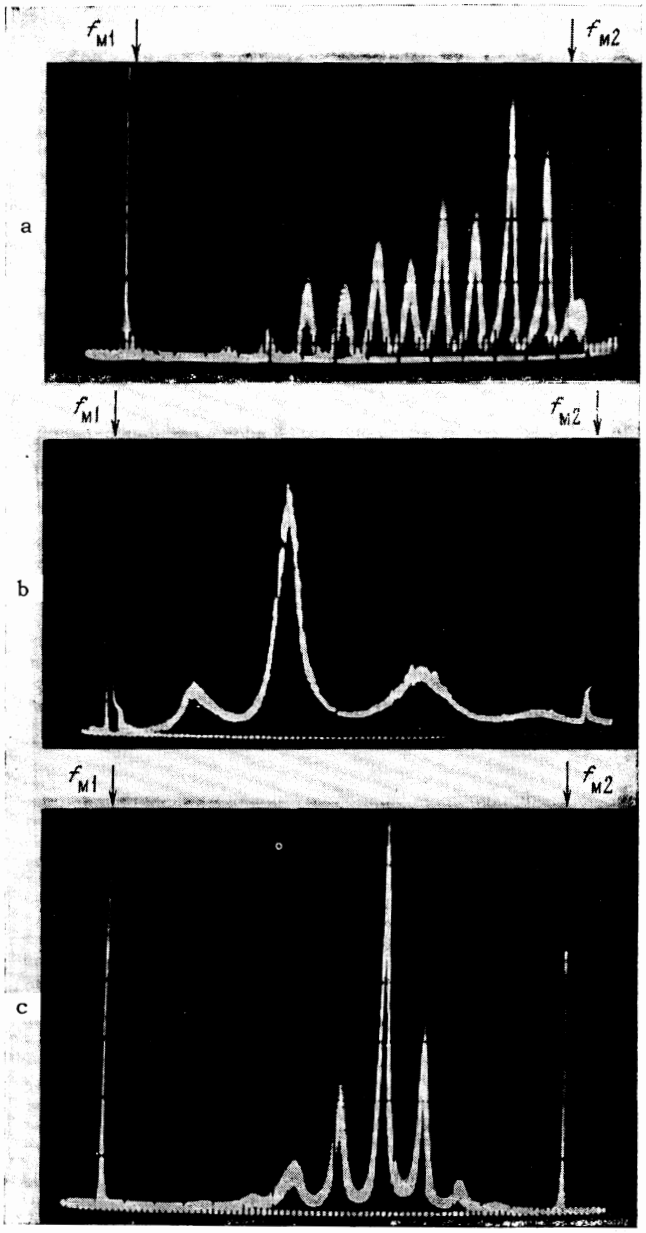

FIG. 2. Typical spectra of high frequency oscillations in the anode current (b) and the probe current (a, c). The two high narrow lines to the left and to the right are frequency markers $f_{M_1} = 0$ and f_{M_2} (indicated by arrows). Near the f_{M_1} marker there are low frequency oscillations (b). a) $f_{M_2} = 30$ MHz, $W_1 = 200$ eV, I = 7 mA, p = 7 $\times 10^{-6}$ mm Hg, L = 130 cm; b) $f_{M_2} = 30$ MHz, $W_1 = 500$ eV, I = 51 mA, p = 4 $\times 10^{-6}$ mm Hg, L = 43 cm; c) $f_{M_2} = 16$ MHz, $W_1 = 140$ eV, I = 4 mA, p = 2.4 $\times 10^{-5}$ mm Hg, L = 140 cm.

2. EXPERIMENTAL DATA

In Fig. 2 we show typical spectra of the high-frequency oscillations in the electron beam taken with different beam parameters. These spectra are distinguished by the sharpness, magnitude, and number of local peaks corresponding to individual frequencies, and by the relative magnitudes of these peaks with respect to the background between them. The "sharp" spectra a and c are observed with relatively low currents (I = [illegible]-7 ma) and low beam energies ($W_1 = 100-200$ eV). As I and W_1 are increased the spectrum becomes smeared (Fig. 2b). The distance between the indi-

vidual frequencies increases substantially as W_1 is increased and as L is reduced (additional spectra are shown in Fig. 8).

However, in spite of the indicated quantitative differences the oscillation spectra shown in Fig. 2 exhibit some well-defined general characteristics that may be described as follows: 1) each spectrum has clearly defined peaks at individual frequencies f_n (n = 1, 2, 3, ...); 2) all the gaps between the individual frequencies Δf_n are found to be the same to an accuracy of 10–25%, this difference being equal to the fundamental frequency

$$\Delta f_n = f_n - f_{n-1} = f_1. \qquad (2a)$$

In other words, all of the frequencies f_n (to the accuracy indicated above) are harmonics of the frequency f_1. The experiments show that the general features remain unchanged for all beam parameters so long as the current I is smaller than some limiting current I_{max} at which a virtual cathode is formed in the beam. In all of the cases described here the condition $I < I_{max}$ is satisfied.

In a number of experiments we have also investigated the dependence of the oscillation spectrum on the beam parameters. These experiments indicate that the relation $f_n = n\Delta f$ is almost always satisfied (to the accuracy indicated above) so that it is sufficient to measure Δf in order to obtain the characteristics of the frequency spectrum. This situation facilitates the measurements appreciably since the first harmonic is not always strong enough for measurement.

In Fig. 3 we show the quantity Δf as a function of the velocity of the beam electrons for two values of the beam length: L = 80 cm (a) and L = 150 cm (b). It is evident that in both cases the quantity Δf is proportional to the velocity v and in going from a to b the coefficient of proportionality varies as 1/L. In Fig. 4 we show the dependence of Δf on beam length for two values of the primary electron velocity:

$$v = 1.04 \cdot 10^9 \text{ cm/sec}(a); \quad v = 0.73 \cdot 10^9 \text{ cm/sec (b)}$$

It is evident that in both cases Δf is inversely proportional to the length of the beam 1/L and in going from a to b the coefficient of proportionality varies approximately as v.

Thus, from Figs. 3 and 4 and Eq. (2a) it follows that

$$\Delta f = C_1 v / L, \quad f_n = C_1 n v / L, \qquad (2b)$$

where C_1 is a coefficient which, in general, depends on the beam density, the plasma density, and the velocity spread of the beam.

It has been found experimentally that Δf is a

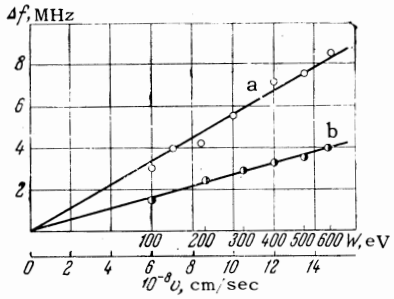

FIG. 3. The dependence of Δf on the velocity of the primary electrons for two values of beam length: curve a for L = 80 cm, curve b for L = 150 cm. The hydrogen pressure $p = 2 \times 10^{-5}$ mm Hg.

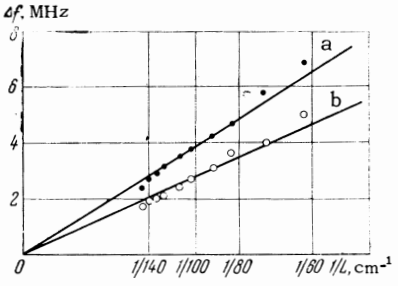

FIG. 4. The dependence of Δf on the reciprocal beam length for two values of the energy of the primary electrons: a) for W_1 = 300 eV, b) for W_1 = 150 eV; $p = 1.8 \times 10^{-5}$ mm Hg.

relatively weak function of the gas pressure: as the hydrogen pressure is increased from $p = 3 \times 10^{-6}$ mm Hg to $p = 10^{-4}$ mm Hg it is found that Δf increases monotonically, but in different ways, depending on the current and the beam velocity, but usually by no more than a factor of two.

The remaining two parameters, i.e., the beam current and the strength of the magnetic field, seem to act primarily on the details of the spectrum, such details being the amplitude distribution over the harmonics and the sharpness of the peaks in a region of each harmonic; however, in general the frequencies of the spectra in the high-frequency region examined here are essentially independent of these parameters. In all the figures shown here H = 3000 G.

A number of experiments have been carried out in order to study the conditions under which the oscillations are excited. These conditions can be summarized as follows. First, the beam length L must exceed some critical value L_c, which is 20–40 cm under the present experimental conditions. Starting with $L = L_c$ increasing L increases the amplitude of the oscillations (for example up to $L \approx 75$ cm); thereafter there is a smooth decay. Second, the beam current must exceed the critical current

$$I \geq I_c. \qquad (3)$$

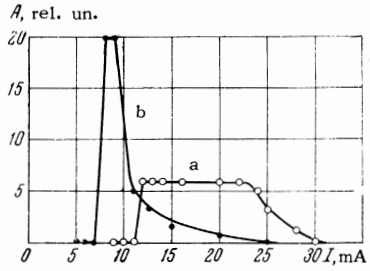

FIG. 5. The dependence of the amplitude of one of the harmonics f = 16 MHz in the probe current on beam current for two values of the hydrogen pressure: curve a for p = 5 $\times 10^{-6}$ mm Hg; curve b for 3×10^{-5} mm Hg; W_1 = 300 eV, L = 135 cm.

This feature is illustrated in Fig. 5 in which we show the amplitude of the oscillations of the probe current as a function of beam current for a given harmonic n = 5 and electron energy W_1 = 300 eV for two values of the hydrogen pressure: a) p = 5×10^{-6} mm Hg b) p = 3×10^{-5} mm Hg. The quantity I_c is a relatively weak function of the harmonic number. It is evident that I_c is reduced as the gas pressure increases. The critical current is a very sensitive function of the velocity of the beam electrons. It is evident from Fig. 6 that this dependence is given by the relation

$$I_c \sim v^3. \qquad (3a)$$

In this sense we can speak of a critical beam velocity v_c and a critical pressure p_c; if the oscillations are to be excited it is necessary that $p > p_c$, $v < v_c$.

If the excitation conditions are satisfied changing the beam parameters only effects the various harmonic amplitudes and the distribution. For example, when the gas pressure is increased the entire spectrum in Fig. 2 is shifted to the right: the harmonic number corresponding to the maximum amplitude is increased and the magnitude of this

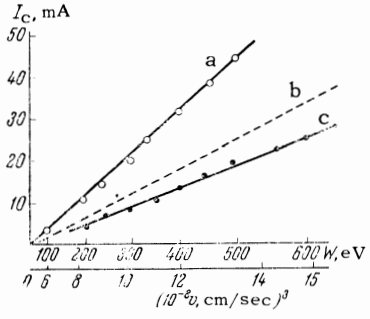

FIG. 6. The dependence of critical current on the cube of the velocity of the primary electrons for two values of the hydrogen pressure: a) for p = 2.4×10^{-6} mm Hg; b) for 3×10^{-5} mm Hg; c) theoretical dependence; W_1 is the electron energy in the beam, L = 150 cm.

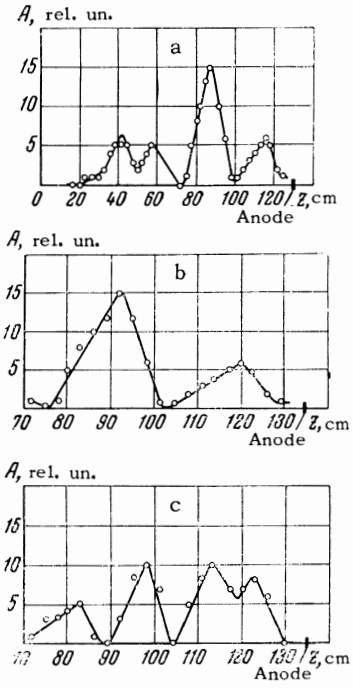

FIG. 7. Dependence of the amplitude of a given harmonic in the probe current on distance between the probe and the cathode: a) and b) n = 5, f = 10 MHz; c) n = 8, f = 16 MHz, W_1 = 300 eV, I = 20 mA, L = 135 cm, p = 3.2×10^{-5} mm Hg.

maximum is increased. The distribution of amplitudes over harmonics is also sensitive to beam current and electron energy.

In Fig. 7a we show the amplitude for a given harmonic n = 5 taken with the probe located at the beam axis as a function of the distance from the cathode (the beam length is fixed L = 135 cm). It is evident that the amplitude of the oscillations exhibits a well-defined periodicity along the length of the beam. One finds that the spatial period, half the wavelength $\lambda_n/2$, for n = 5 is 25–28 cm, that is to say, the relation $\lambda_n/2 = \lambda/n$ is satisfied.

In Figs. 7b and 7c the variation in amplitude along the length of the beam is compared for two harmonics: n = 5 (b) and n = 8 (c). (This comparison is made only for the second half of the beam (70 cm $\leq$ L $\leq$ 135 cm) where the amplitudes of both harmonics are large.) It is evident that the spatial periods for these harmonics are 25–27 cm for n = 5 and 15–17 cm for n = 8, i.e., in the ratio L/5 and L/8.

Thus the data in Fig. 7 indicate that the wavelengths for the various harmonics are related to the beam length by Eq. (1).

It has been shown by Fedorchenko et al.[10] that the secondary electrons ejected from the anode by the beam play an important role in the excitation of high-frequency oscillations in an electron beam.

In order to investigate the extent to which this

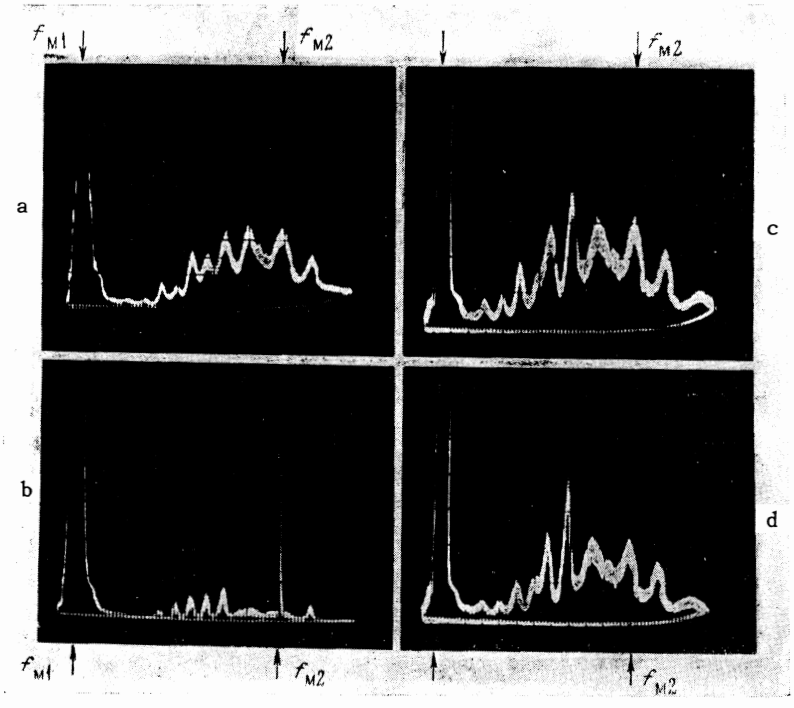

FIG. 8. The spectra of current oscillations to the Langmuir probe for two values of the anode potential and two values of the hydrogen pressure: W_1 = 350 eV, I =30 mA, L = 150 cm. The arrows below the figure indicate the frequency markers f_{M1} = 0 and f_{M2} = 30 MHz. a) φ_a = 0, p = 3×10^{-6} mm Hg, b) φ_a = 50 V, p = 3×10^{-6} mm Hg, c) φ_a = 0, p = 1×10^{-5} mm Hg, d) φ_a = 50 V, p = 1×10^{-5} mm Hg. Strong low-frequency oscillations are visible near the marker f_{M1} = 0.

phenomenon is of importance in the present experiments we have carried out an experiment similar to that reported in [10] with the single difference that it was carried out at different gas pressures so that it was possible to control the electron density produced by ionization due to the beam. In this experiment a grounded high transmission grid (square cells 1 mm on a side made from tungsten wire 0.1 mm in diameter) is located in front of the anode; at the same time a positive potential ($\varphi_a \approx 50$ V) is applied to the anode in order to suppress secondary electrons.

In Figs. 8a and 8b we show the oscillation spectrum obtained at the Langmuir probe (at the center of the beam) for two values of the anode potential: $\varphi_a = 0$ and $\varphi_a = 50$ V with a rather small residual gas pressure p = 3×10^{-6} mm Hg. It is evident that under these conditions the inhibition of the secondary emission causes a very strong reduction in the amplitude of the oscillations.

However, the effect of secondary emission from the anode on the oscillation amplitude is important only at low gas pressures ($p \lesssim 3-5 \times 10^{-6}$ mm Hg); when the gas pressure is increased the importance of this effect is diminished rapidly and starting at $p \approx 1-1.5 \times 10^{-5}$ mm Hg its effect becomes negligibly small (Figs. 8c, d). This means that the effect of the secondary electron emission from the anode on the excitation of oscillations is important only when the density of these electrons is large compared with the density of electrons produced in the gas by the beam, that is to say, when $p \lesssim 3-5 \times 10^{-6}$ mm Hg; the effect disappears when $p \gtrsim 1-1.5 \times 10^{-5}$ mm Hg.

We note that in addition to the high-frequency oscillations described above there are also relatively low frequency oscillations at single frequencies from fractions of a megahertz up to 1–1.5 MHz. These oscillations are evident, in particular, in Figs. 2 and 8. The nature of these oscillations has not been investigated in the present work.

Before discussing the results we present certain data which characterize the energy spectra of the electrons in the beam and the quantity α which is the ratio of the density of plasma electrons formed by the beam to the density of the primary beam. In Fig. 9 we show the velocity distribution of the beam electrons (as determined by the method described in [11]) for an electron energy W_1 = 150 eV and two values of the current: a) I = 5 ma < I_c and b) I = 14 ma > I_c (the current I = 14 ma is somewhat less than this maximum current I_{max} at which a virtual cathode is formed in the beam). For case b we use the mean-value theorem to determine the mean average velocity spread of the beam electrons Δv_{av}. The results are shown in Fig. 9 by the dashed line c. It is evident that $\Delta v_{av} \approx 0.5 v_{av}$. On the basis of these results we assume below that when $I \lesssim I_c$ the quantity $\Delta v \approx 0$ and when $I > I_c$ the ratio $\Delta v / v_{av} \approx 0.5$. As far as the quantity α is concerned we note that the probe estimates similar to those in [12] show that when $p \approx 1 \times 10^{-5}$ mm Hg the quantity $\alpha \approx 1$

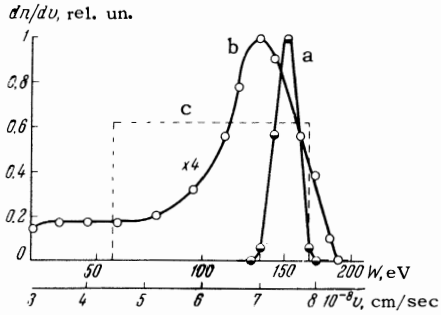

FIG. 9. The velocity distribution of the beam electrons as a function of the electron energy W_1 = 150 eV and two values of the beam current: curve a for I = 5 mA and curve b for I = 14 mA. The dashed line c indicates the method of estimating the average velocity spread in the beam. L = 50 cm, p = 4×10^{-6} mm Hg. The case denoted by b is distinguished from a by a much larger oscillation amplitude and beam current (in a these oscillations are not observed).

and when p is increased to 10^{-4} mm Hg we find that α increases monotonically but never exceeds a value of 4–5.

3. DISCUSSION OF RESULTS

It is well known[1-7] that the oscillation properties of a uniform system of charged particles consisting of a monoenergetic electron beam and a cold plasma can be characterized with respect to longitudinal oscillations (neglecting the thermal motion of particles) by the dispersion relation

$$\omega_+^2/\omega^2 + \omega_2^2/\omega^2 + \omega_1^2/(\omega - kv)^2 = 1, \qquad (4)$$

where ω is the angular oscillation frequency; $k = 2\pi/\lambda$ is the wave number; v is the beam velocity; ω_+, ω_2 and ω_1 are respectively the frequencies of the characteristic ion oscillations, the oscillations of the plasma electrons, and the beam electrons.

The consequences of Eq. (4) are found to be very different depending on the ratio between the oscillation wavelength λ and the transverse dimensions (radius) of the system r_0 (it is assumed that the transverse dimensions of the primary beam and the plasma are the same). This result is easily seen from the two limiting cases which have been discussed in the introduction: 1) $\lambda \ll r_0$; in this case the quantities ω_+, ω_2 and ω_1 are the Langmuir frequencies (ω_p) of the ions and the electrons:

$$\omega_+ = \omega_{p+} = (4\pi(n_1+n_2)e^2/M_+)^{1/2},$$
$$\omega_1 = \omega_{p1} = (4\pi n_1 e^2/m)^{1/2}, \quad \omega_2 = \omega_{p2} = (4\pi n_2 e^2/m)^{1/2}; \qquad (4a)$$

2) $\lambda \gg r_0$; in this case the quantities ω_+, ω_2 and ω_1 are not the Langmuir frequencies but, as indicated in the introduction, depend on the oscillation wavelength ([3-7]):

$$\omega_+ = \frac{\omega_{p+}}{\sqrt{2}} kr_0\sqrt{\mathcal{L}}; \quad \omega_2 = \frac{\omega_{p2}}{\sqrt{2}} kr_0\sqrt{\mathcal{L}};$$
$$\omega_1 = \frac{\omega_{p1}}{\sqrt{2}} kr_0\sqrt{\mathcal{L}}. \qquad (4b)$$

The quantity $\mathcal{L}$, for the case of a uniformly dense cylindrical beam of radius r_0 propagating in a plasma with the same transverse dimension along the axis of a metal tube of radius R_0 and length L ($L \gg R_0$), is given by an expression of the form[3, 5, 6]

$$\mathcal{L} = \begin{cases} \ln(R_0/r_0) & \text{for } \lambda/2\pi > R_0 \\ \ln(\lambda/2\pi r_0) & \text{for } \lambda/2\pi < R_0 \end{cases} \qquad (4c)$$

In the first of these cases we find that $\mathcal{L} \approx 3.4$ for the present geometry. Under the experimental conditions described here the oscillation wavelength is of the order of tens of centimeters whereas r_0 = 0.5 cm and R_0 = 15 cm. Hence we must use the dispersion relation that applies to the case $\lambda \gg r_0$:

$$\omega_{p+}^2/\omega^2 + \omega_{p2}^2/\omega^2 + \omega_{p1}^2/(\omega - kv)^2 = 2/\mathcal{L}(kr_0)^2. \qquad (4d)$$

A similar relation has been obtained in [13] except that the quantity $\mathcal{L}$ is replaced by a tabulated function which is equal to it numerically.

We note that it is assumed everywhere that the motion of particles across the beam can be neglected; this is equivalent to the assumption that a rather strong magnetic field acts along the beam ($\omega_H = eH/mc \gg \omega$).

If the beam is not monoenergetic, the "beam" term which appears in the dispersion relation assumes the form

$$\omega_{1p}^2 \int_{-\infty}^{+\infty} \frac{f(v)\,dv}{(\omega - kv)^2},$$

where f(v) is the distribution function giving the velocity of the beam electrons. If f(v) is rectangular over some velocity interval (as in Fig. 9) case c) then f(v) ≈ const within this interval and f(v) ≈ 0 outside so that it is evident that the term $\omega_{1p}^2/(\omega - kv)^2$ in the dispersion relation is replaced by the term

$$\omega_{1p}^2/[\omega - k(v - \Delta v)][\omega - kv].$$

If the density of plasma electrons is not too small compared with the ion density the first term in the right side of (4d) can be neglected as compared with the second. Under these conditions we find

$$F\left(\frac{\omega}{k}\right) \equiv \frac{\omega_{2p}^2}{(\omega/k)^2} + \frac{\omega_{1p}^2}{[\omega/k-(v-\Delta v)][\omega/k-v]} = \frac{2}{\mathcal{L} r_0^2}. \tag{5}$$

In order to simplify the subsequent analysis we shall use the value 3.4 for $\mathcal{L}$; in this case the right side of Eq. (5) becomes a constant equal to 2.5 regardless of the oscillation wavelength.

When $\Delta v < v$ Eq. (5) becomes a fourth-order equation in ω/k and, depending on the system parameters, (for real k) can have either real or complex roots; in the latter case oscillations are excited. The function $F(\omega/k)$ and the line $F(\omega/k)$ = const are shown for the case $\Delta v < v$ in Figs. 10a–c; the case $\Delta v = v$ is shown in Fig. 10d.

In cases a and c the line $F(\omega/k)$ = const intersects branches of the function $F(\omega/k)$ at four points; this means that all four roots of Eq. (5) correspond to real ω, that is to say, the system is stable. In case b, where there are two points of intersection, only two of the roots are real and the other two (complex conjugates) roots have positive imaginary parts corresponding to instability (excitation).

In the case shown in Fig. 10d, $\Delta v = v$ and Eq. (5) degenerates into a third order equation which only has real roots ω. Everywhere below we consider the case $\Delta v < v$.

It is evident that the instability is possible on two branches of the dispersion equation: the left branch $[0 < \omega < k(v - \Delta v)$ and the right branch $(k(v - \Delta v) < \omega < kv]$.

The instability on the left branch of the function $F(\omega/k)$, the transition a → b in Fig. 10, can be realized by any one of four methods: 1) increasing the beam current, 2) increasing the plasma density, 3) reducing the velocity of the beam electrons v, and 4) increasing the velocity spread Δv (under the condition that $\Delta v < v$).

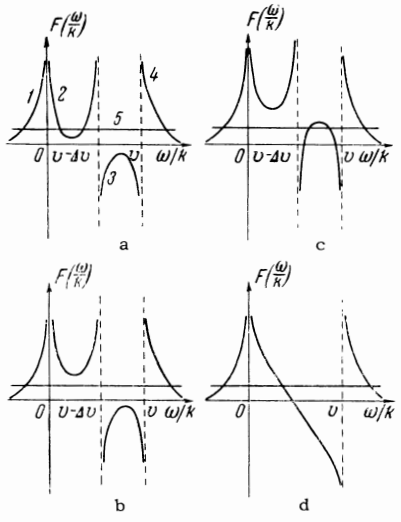

FIG. 10. Dispersion curves: a, b, c) $\Delta v < v$; d) $\Delta v = v$. Curve 2 is the left branch of the function $F(\omega/k)$, 3) the right branch of this function, 5) the line $F(\omega/k)$ = const. The cases denoted by a, c and d correspond to stability and b instability.

In order to provide a qualitative comparison of this theory and the experiment in Eq. (4d) we write $\Delta v = 0$ (in this case branch 3 in Fig. 10 disappears and the oscillatory properties of the system can be described by the relative positions of branches 2 and 5). Setting the derivative with respect to ω/k equal to zero for the left side of the equation we find the abscissa of the point of tangency of branches 2 and 5 of the function $F(\omega/k)$:

$$\omega = \frac{kv}{1+(\alpha+m/M)^{-1/3}}, \tag{2c}$$

where $\alpha = n_2/n_1$. When $\alpha >> m/M$ the oscillations are true electron oscillations. Substituting this expression in Eq. (5) we find the critical beam current for which branch 2 in Fig. 10 breaks away from branch 5, that is to say, the point at which oscillations are excited:

$$I_c = \frac{mvr_0^2}{4e}(\omega_{1p})_c^2 = \frac{mv^3}{2e\mathcal{L}[1+(\alpha+m/M)^{1/3}]^3} \tag{3b}$$

where $\mathcal{L}$ is the quantity given by Eq. (4c); for example, with $mv^2/2 = W_1 = 500$ eV the critical beam current $I_c \approx 30$ ma.

In computing I_c we have taken $\Delta v = 0$. This approximation is justified as follows: when $I < I_c$ the velocity spread of the beam is actually very small (cf. curve a in Fig. 9) and when $I > I_c$ it is determined by the oscillations that have already developed.

Now let us compare the expressions in (2c) and (3b) for the oscillation frequency spectrum and the critical current with the experimental data. It is evident from Eq. (2c) that at least close to the critical current ($I \gtrsim I_c$) the oscillation frequency is proportional to the product kv. As far as the quantity k is concerned it is reasonable to assume that in our case, in which the beam is bounded in length by the metal electrodes, the longitudinal waves of the electric field will be reflected from these electrodes so that standing waves will be set up in the system. If this is the case those modes will be excited for which the wavelength λ is equal to one of the characteristic values of the system λ_n:

$$\lambda = \lambda_n = 2L/n \quad \text{or} \quad k = 2\pi/\lambda = n\pi/L, \qquad n = 1, 2, 3, \ldots, \tag{1a}$$

while modes that do not satisfy this relation will be quenched as a consequence of successive re-

flections from the end plates (a similar assumption has been made in the theoretical papers[14, 15]). Under these conditions the oscillation spectrum will be given by

$$\omega = \omega_n \approx \pi \frac{v}{L} n \frac{1}{1+\alpha^{-1/3}} \qquad (2d)$$

(for $\alpha \gg m/M$).

It is evident from Eq. (2d) that $\omega_n \sim n,\ v,\ 1/L$. This is precisely the spectrum that has been observed in the experiment (cf. Fig. 2-4). For constant values of n, v and L the oscillation spectrum (2d) does not depend on the beam current and must increase somewhat with increasing α, that is to say, with increasing gas pressure; for example, when the quantity α is increased from 1 to 10 we find that ω_n increases by a factor of 1.4 in accordance with Eq. (2d). These conclusions are also in good agreement with the experimental data given above.

We have already indicated that the oscillations characterized by different n are not exact harmonics in frequency although the frequency deviation from exact harmonics is small, being of the order of 10–25%. It is our opinion that this feature is due to some geometrical effect and other beam parameters but that it is evidently not of fundamental importance.

Let us now consider the critical current (3b). The function $I_c(v^3)$ is plotted by the dashed line c in Fig. 6 for $\alpha = 1$. In the same figure we show the experimental data for two gas pressures. It is evident that the theoretical function $I_c(v^3)$ is very close to the experimental function. If it is assumed that the quantity α is somewhat less than unity on curve a, then on curve b it is somewhat larger and we not only obtain qualitative agreement but even quantitative agreement between theory and experiment (as far as the actual value of α is concerned we have already noted that it is not very different from unity).

It should also be noted that Eq. (3b) predicts that I_c in our case must be a relatively weak function of λ, that is to say, a weak function of the harmonic number in the spectrum. This feature is also in good agreement with the experimental results.

The comparison given above indicates that the oscillations observed in these experiments are longitudinal electron oscillations and that they are described by the dispersion equation (4)–(5) as supplemented by the standing wave condition (1).

It is of interest to consider the case $\alpha = 0$: the electron beam is exactly balanced by the ions and there are no plasma electrons. In this case Eq. (2c) describes the electron-ion oscillations considered by Buneman.[16] Under these conditions it is found that the critical current I_c given by Eq. (3b) for $\alpha = 0$ is essentially the same as the limiting current I_l starting with which pure electron oscillations are excited, this being the instability described by Pierce which leads to the formation of a virtual cathode.[17] [1)]

If plasma electrons are introduced into the beam (with an equal number of ions), that is to say, if the quantity α is increased, the current I_c is reduced in accordance with Eq. (3b) and the quantities I_c and I_l are no longer the same. Under the conditions reported in these experiments I_c is several times smaller than I_l.

Up to this point we have considered the instability of the beam on the left branch of the function $F(\omega/k)$ (curve 2 in Fig. 10). If the plasma density becomes large enough this branch will always be detached from the line $F(\omega/k) = \text{const}$ and the stability of the beam is then determined by the right branch of $F(\omega/k)$ (curve 3 in Fig. 10). In this case raising the plasma density with all other conditions remaining the same will sooner or later cause the system to become stable (the transition b → c in Fig. 10). It is evident from Eq. (5) that this situation obtains when

$$\alpha \equiv \frac{\omega_2^2}{\omega_1^2} \equiv \frac{n_2}{n_1} \geqslant \left(2\frac{v}{\Delta v} - 1\right)^2 + \frac{0.6v^2}{r_0^2\omega_1^2}\left(1 - \frac{\Delta v}{2v}\right)^2, \qquad (6)$$

where n_1 and n_2 are respectively the beam density and the plasma density (here we assume that $\lambda/2\pi > R_0$ and $\mathcal{L} = \ln(R_0/r_0) = 3.4$). When $\Delta v = 0.5v$ the condition in (6) implies

$$\alpha > 9 + 0.35\,(v/\omega_1 r_0)^2, \qquad (6a)$$

that is to say $\alpha \gtrsim 10$–25. If the stability of the system is determined by the right branch of $F(\omega/k)$ the critical current must increase with increasing plasma density. However, as we have already noted above, in the present experiments this feature is not observed since α is usually of the order of unity (rarely 2–3) and the instability is determined by the left root of $F(\omega/k)$.

In order to make a more detailed comparison of the theory and experiment the frequency spectrum was computed on an electronic computer. In this case, in order to facilitate the calculations the real

[1)] As is well known, [16], [17] these instabilities exhibit an important difference: both the electrons and the ions participate in the Buneman oscillations whereas the Pierce instability develops with the ions at rest; this result is connected with the fact that the electric fields of the charges induced in the metal walls that surround the beam randomly excite potential fluctuations in the beam and when $I > I_l$ the initial fluctuation is amplified.

velocity distribution of the beam electrons (Fig. 9, curve b) is replaced by a rectangular distribution (Fig. 9, curve c). The validity of this substitution is justified by the result: it is found (cf. below) that taking account of the strong velocity spread in the beam [$\Delta v = 0.5-0.8\,v$] only leads to small quantitative corrections that cannot really effect a comparison of the theory and experiment.

The determination of the real and imaginary parts of the oscillation frequency $\omega = \omega_r + i\gamma$ was carried out by A. E. Bazhanova on an electronic computer. In this case we have also found the values of the critical current starting with which the condition $|\gamma| > 0$ is satisfied.

The results of these calculations are shown in most complete form in Fig. 11 where the plasma density n_2 is plotted along the abscissa axis while the quantities ω_r/kv_{av} and γ/kv_{av} are plotted along the ordinate axis. The curves in Fig. 11 are plotted for two values of the electron velocity: $v = 1.8 \times 10^9$ cm/sec (a) and $v = 1 \times 10^9$ cm/sec (b) and two values of the beam current: I = 100 mA (dashed curves) and I = 20 mA (solid curves). In order to expand the range of the parameters n_1, n_2 and v in which $|\gamma| > 0$, the quantity Δv, which characterizes the velocity spread in the beam in Fig. 11, is not taken to be constant, but changes monotonically going from left to right, varying from the value 0.8 v to the value 0.5 v.

The following conclusions follow from Fig. 11.

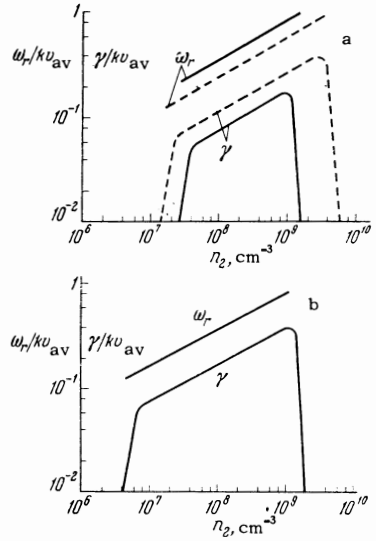

FIG. 11. The quantity ω_r/kv_{av} and the quantity γ/kv_{av} as functions of the plasma density n_2: a) for a beam velocity $v = 1.8 \times 10^9$ cm/sec; the solid curves hold for I = 20 mA and $n_1 = 5.5 \times 10^8$ cm^{-3} and the dashed curves for I = 100 mA and $n_1 = 5.5 \times 10^8$ cm^{-3}; b) for a beam velocity $v = 1 \times 10^9$ cm/sec, I = 20 mA, $n_1 = 2 \times 10^8$ cm^{-3}. $v_{av} = v - \Delta v/2$.

1. The oscillation frequency is proproportional to kv_{av}, the coefficient of proportionality being of the order of several tenths; as the plasma density increases this coefficient slowly approaches unity. The oscillation frequency is a weak function of beam density. When $k = n\pi/L$ (2) the oscillation spectrum is given by $\omega_n \sim vn/L$ (n = 1, 2, 3, ...).

2. For fixed density and mean velocity oscillations are only excited ($|\gamma| > 0$) within certain ranges of plasma density: from $n_2 = n_{2min} \approx (1/30)n_1$ to $n_2 = n_{2max} \approx (12-25)n_1$ and as v is reduced this range is shifted to the left. The physical meaning of this phenomenon was explained at the beginning of the present section and stems from the fact that when $n_2 < n_{2min}$ the case in Fig. 10a is realized and when $n_2 > n_{2max}$ the case in 10c is realized.

3. For a fixed plasma density oscillations are only excited if the beam current exceeds some critical value that increases with increasing beam velocity.

It is evident that these conclusions are in good qualitative agreement with the experimental results described above. A quantitative comparison of these results with the experimental data is given in Figs. 3 and 4. The lines plotted on these figures are obtained by multiplying the computed function $f_1(v)$ and $f_1(1/L)$ by constant coefficients that are respectively 1.7 and 1.2.

Introducing these correction coefficients was found to be sufficient for complete quantitative agreement between the theoretical predictions and the experimental data. In order to facilitate the calculations we have made a number of simplifying assumptions above such as the uniformity of the beam density and the plasma density in the transverse and longitudinal directions, the absence of transverse particle motion, a rectangular energy spectrum for the primary electrons, and the assumption that under the conditions shown in Figs. 3–6 $\alpha = 1$ and $\Delta v/v = 0.5$ (only approximately); the fact that the theory and experiment agree so well is, in our opinion, to be taken as rather good experimental verification of the theory.

One further result shown in Fig. 11 is noteworthy: the oscillation growth rate γ is also proportional to kv_{av}. In particular, this means that when $I > I_c$ the short waves are excited more efficiently than the long waves and one expects that the oscillation amplitude will increase with increasing harmonic number. On the other hand, waves that are too short ($\lambda/2\pi < R_0$) can only be excited with difficulty because in accordance with Eqs. (3b) and (4c), when $\lambda/2\pi < R_0$ the critical current increases as the wavelength is reduced.

These two factors are evidently responsible for the nature of the observed experimental distribution of amplitude over harmonics, that is to say, the presence of a maximum amplitude at some mean harmonic number n which increases with increasing plasma density.

It is interesting to consider one further fact with regard to the oscillation amplitude: when $L < L_c$ the coherent oscillations are not observed ($L_c \approx 20-40$ cm). This result evidently follows from two circumstances. First of all, the instability of a beam which traverses a quiescent plasma is a convective instability; hence, the amplitude of the oscillations increases along the length of the beam and in order to reach the required magnitude the beam length L must be greater than some critical value.[8, 18] Secondly, as L increases the total number of ions produced in the gas by the beam also increases so that the plasma density increases. In this latter sense the quantity L has the same physical meaning as a critical plasma density.

Let us consider the basic results observed in these experiments: 1) the discrete oscillation spectrum; 2) the fact that the frequencies are related as harmonics $f_n \sim nv/L$ and the wavelengths as $\lambda_n \sim L/n$; 3) the characteristic dependence of frequency on beam density and plasma density; 4) the fact that the critical current increases approximately as v^3 and that it is reduced with increasing α etc.; these are all (both qualitatively and quantitatively) described by the dispersion equation (5) for longitudinal electron oscillations supplemented by the standing wave condition (1). In other words, the totality of experimental data obtained here is in good agreement with the theoretical predictions for the development of an "ordinary" beam instability in a system of finite dimensions.

As we have already indicated in the introduction, the oscillations studied here differ substantially from Langmuir oscillations both in spectrum and in the fact that they are excited only when the beam density n_1 is not negligibly small compared with the plasma density n_2. The frequencies of the observed oscillations are of the order of 10^7 Hz, that is to say, orders of magnitude lower than the Langmuir frequency $f_{p2} = \omega_{p2}/2\pi$. If the plasma density is increased substantially (by increasing the gas pressure) then, as we have indicated above, the maximum oscillation amplitude is shifted toward higher frequencies (shorter wavelengths). This evidently is an expression of the tendency toward a gradual transition of these oscillations into Langmuir oscillations. There is reason to believe that with a significant increase in n_2/n_1 the long wave oscillations will be damped and only Langmuir oscillations will be excited, as is the case in a rarefied beam passing through a dense plasma (cf. [8]).

The authors wish to thank Ya. B. Faĭnberg for his interest and for valuable discussions and A. E. Bazhanova for calculating the roots of the dispersion equation with an electronic computer.

[1] Ya. B. Fainberg, Atomnaya energiya (Atomic Energy) **11**, 313 (1961).

[2] A. A. Vedenov, E. P. Velikhov and R. Z. Sagdeev, UFN **73**, 701 (1961), Soviet Phys. Uspekhi **4**, 332 (1961).

[3] G. I. Budker, Atomnaya energiya (Atomic Energy) **5**, 9 (1956).

[4] G. I. Linhart, Plasma Physics, North Holland, Amsterdam, 1960.

[5] D. Finkelstein and P. Sturrock in Plasma Physics, ed. J. E. Drummond, McGraw-Hill, New York, 1961, Chap. 8.

[6] M. F. Gorbatenko, Coll. Fizika plazmy i problemy ypravlyaemogo termoyadernogo sinteza (Plasma Physics and the Problem of Controlled Thermonuclear Fusion), Acad. Sci. Uk. S.S.R., Kiev, 1962; Ukr. fiz. zhurn. **7**, 233 (1962).

[7] R. Briggs, Electron-stream Interactions with Plasma, MIT Press, Cambridge, 1964.

[8] I. F. Kharchenko, Ya. B. Faĭnberg, R. M. Nikolaev, E. A. Kornilov, E. A. Lutsenko, and N. S. Pedenko, JETP **38**, 685 (1960), Soviet Phys. JETP **11**, 493 (1960).

[9] C. C. Cutler, Proc. I.R.E. **44**, 61 (1956).

[10] V. D. Fedorchenko, V. I. Muratov and B. N. Rutkevich, ZhTF **34**, 458 (1964), Soviet Phys. Tech. Phys. **9**, 358 (1964).

[11] M. V. Nezlin, JETP **46**, 36 (1964), Soviet Phys. JETP **19**, 26 (1964).

[12] M. V. Nezlin and A. M. Solntsev, JETP **48**, 1237 (1965), Soviet Phys. JETP **21**, 836 (1965).

[13] M. Yoshikawa, Nuclear Fusion, **1**, 167 (1961).

[14] M. A. Lampert, J. Appl. Phys. **27**, 5 (1956).

[15] M. Sumi, J. Phys. Soc. Japan **13**, 1476 (1958).

[16] O. Buneman, Phys. Rev. **115**, 503 (1959).

[17] J. R. Pierce, J. Appl. Phys. **15**, 721 (1944).

[18] P. A. Sturrock, Phys. Rev. **117**, 1426 (1960).

Translated by H. Lashinsky
48